Advanced Robotics, Vol. 20, No. 11, pp. 1281–1301 (2006)

Also available online - www.brill.nl/ar

Full paper

Nano encoders based on vertical arrays of individual carbon nanotubes

LIXIN DONG [1], ARUNKUMAR SUBRAMANIAN [1], DANIEL HUGENTOBLER [1], BRADLEY J. NELSON [1,*] and YU SUN [2]

[1] *Institute of Robotics and Intelligent Systems, ETH Zurich, 8092, Zurich, Switzerland*
[2] *Department of Mechanical and Industrial Engineering, University of Toronto, Toronto, Canada*

Received 27 April 2006; accepted 9 July 2006

Abstract—Linear encoders for nanoscale position sensing based on vertical arrays of individual carbon nanotubes are presented. Vertical arrays of single multi-walled carbon nanotubes (MWNTs) are realized using a combination of electron beam lithography (EBL) and plasma-enhanced chemical vapour deposition growth. EBL is used to define 50- to 150-nm nickel catalyst dots at precise locations on a silicon chip. Precise control of the position, density and alignment of the tubes has been achieved. Aligned nanotube arrays with spacing varying from 250 nm to 25 μm are realized. Field emission properties of the array are investigated inside a scanning electron microscope equipped with a 3-d.o.f. nanorobotic manipulator with nanometer resolution functioning as a scanning anode. With this scanning anode and the single MWNT array, a nano encoder is investigated experimentally. Vertical position is detected by the change in emission current, whereas the horizontal position of the scanning anode is sensed from the emission distribution. A resolution of 98.3 nm in the vertical direction and 38.0 nm (best: 12.9 nm) in the lateral direction has been achieved.

Keywords: Carbon nanotube array; field emission; nano encoder; nanorobotic manipulator; scanning anode.

1. INTRODUCTION

In electric servomotors, encoders play a significant role by providing precision angular or linear position sensing feedback. Similarly, with the development of nano machines [1–4] nanometer-scale position sensing with nanometer-sized devices is required for their successful application.

To shrink the sizes of conventional optical encoders, different measurement principles must be considered. Although tunneling current and laser-deflection techniques can provide extremely high resolution [5, 6], the effective distance of

*To whom correspondence should be addressed. E-mail: bnelson@ethz.ch

the former is less than 1 nm and the latter generally involves a complex laser apparatus. Another possible feedback mechanism is to use the interlayer resistance of a telescoping multi-walled carbon nanotube (MWNT) for position sensing [7]. The potential for quantized interlayer conductance can result in resolutions at atomic lattice levels [8]. On the other hand, the dependence of field emission currents on inter-electrode distance has shown promise for non-contact position sensing [9, 10]. Recent results with individual nanotube emitters and telescoping nanotubes have shown the feasibility of this method [11, 12]. Moreover, the energy distribution around a field emitter [13, 14] is a potential technique for lateral position sensing.

Plasma-enhanced chemical vapour deposition (PECVD) has been successfully used for the growth of individual MWNTs from nickel catalyst nanodots defined by electron beam lithography (EBL) [13]. In this paper, we present a nano encoder based on vertically-aligned single MWNT emitters grown with this technique. Vertical and lateral position sensing are investigated from experimental, theoretical and design perspectives.

In the following, directed growth of single MWNT arrays is introduced in Section 2. The design and operating principle of nano encoders is presented in Section 3. A nanomanipulation-based scanning anode technique for field emission property characterization is shown in Section 4 and the basic field emission property of an individual tube in the array is measured. In Section 5, experiments with single MWNT array-based linear nano encoders are described.

2. DIRECTED GROWTH OF SINGLE MWNT ARRAYS

Vertically aligned MWNTs were realized using a combination of EBL and PECVD growth of MWNTs. EBL was used to define 50- to 150-nm nickel catalyst dots at precise locations on a silicon chip. Next, vertically aligned nanotubes were grown by PECVD at Nanolab (USA). Precise control of the position, density and alignment of the tubes has been achieved. Aligned nanotube arrays with spacing varying from 250 nm to 25 μm were realized. Figure 1 shows vertically-aligned MWNTs grown by this technique.

3. DESIGN AND PRINCIPLE OF NANO ENCODERS

3.1. Structure

A single carbon nanotube (CNT) array-based nano encoder is designed as shown in Fig. 2. A scanning anode is placed on a moving body and its position detected by monitoring the field emission current from the CNT emitter array.

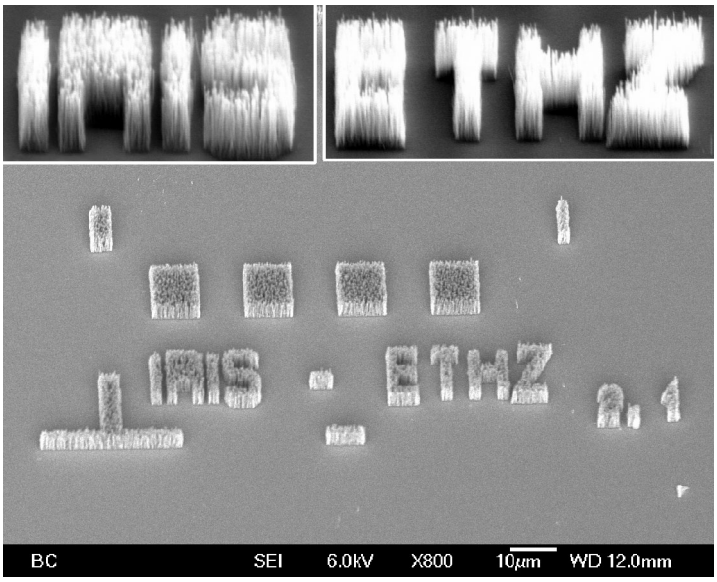

(a)

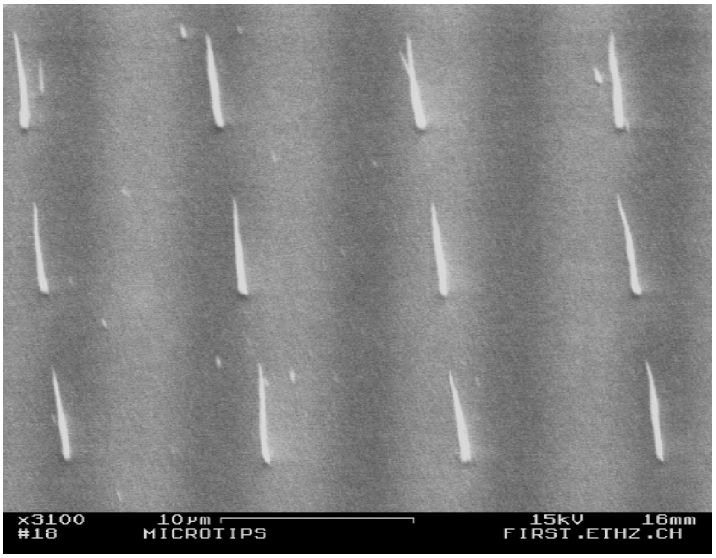

(b)

Figure 1. Single MWNT arrays: (a) 250-nm to 1-μm spacing (insets show logos 'IRIS' and 'ETHZ' in pseudo-colors observed at a 45° tilt angle), (b) 10-μm spacing 3 × 4 array of single MWNTs, (c) 25-μm spacing 3 × 3 array of single MWNTs and (d) an individual tube in the array. (Scale bars: 10 μm.)

3.2. Vertical position sensing

Field emission from a nanotube emitter is governed by the Fowler–Nordheim (F–N) theory [15]. This theory, originally published in 1928, was the first generally

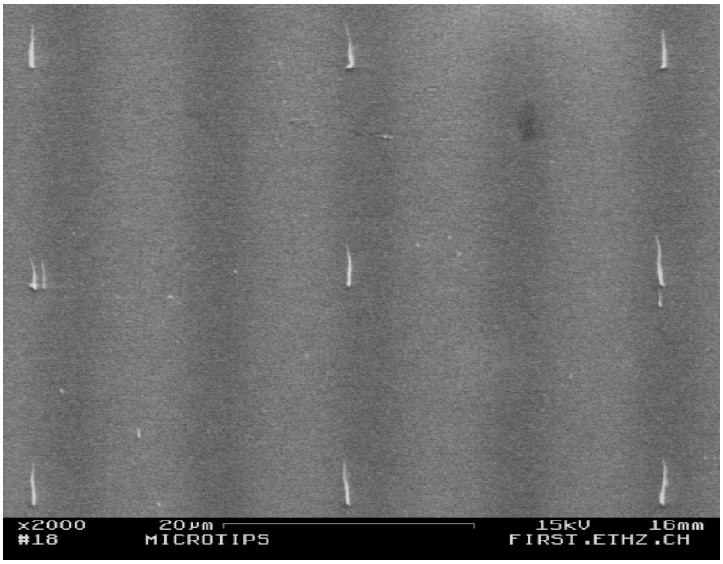

(c)

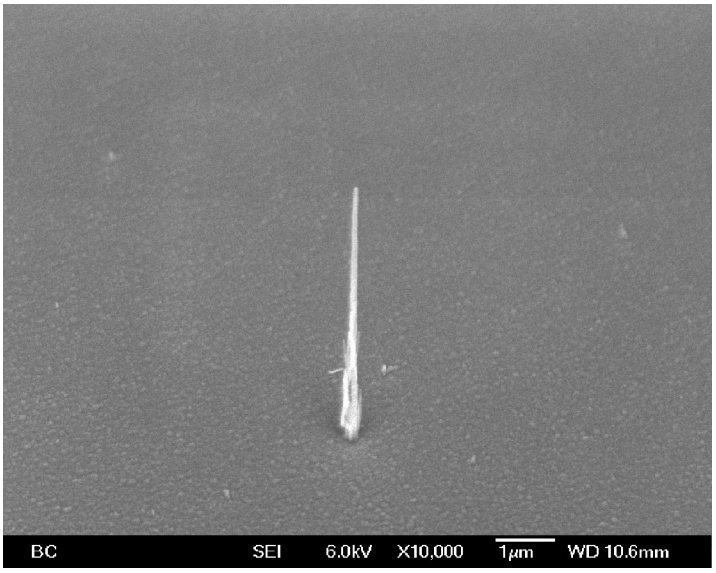

(d)

Figure 1. (Continued).

accepted explanation of field emission in terms of the newly developed theory of quantum mechanics. The first experimental research on CNT field emission demonstrated that nanotubes obey this theory [16]. According to the F–N theory, the field emission current density j is a function of the electric field E and the emitter

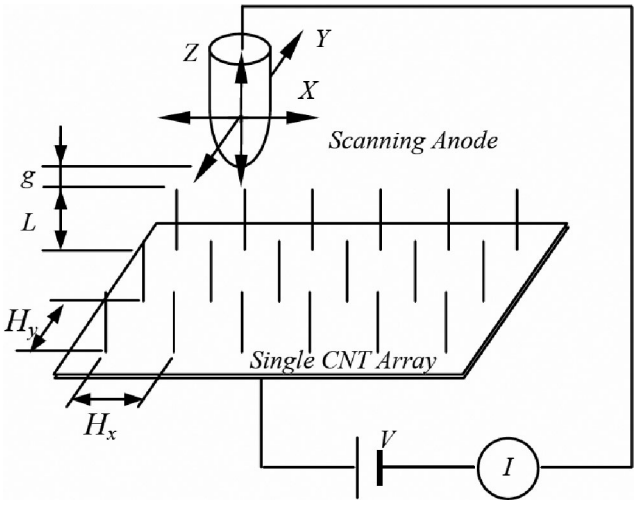

Figure 2. Nano encoder consisting of a scanning anode field emission probe and a single nanotube array. L is the length of the tubes, H_x and H_y the spacing between tubes in the x and y direction, and g the inter-electrode (anode probe–tube tip) distance.

work function Φ:

$$j = \frac{e^3}{4(2\pi)^2\hbar\Phi} E^2 \exp\left(-\frac{4\sqrt{2m_e}}{3\hbar eE}\Phi^{3/2}\right), \tag{1}$$

where e is the elementary positive charge, m_e is the electron mass, $\hbar$ is Planck's constant and $\hbar = h/2\pi$.

The emission current can then be expressed as [15]:

$$I = 1.54 \times 10^{-6} \frac{AL^2V^2}{G^2r^2\Phi} \exp\left(-6.79 \times 10^7 \frac{\Phi^{3/2}Gr}{VL}\right), \tag{2}$$

where I is the emission current (A), V is the applied voltage (V), Φ is the work function of the nanotube tip (eV), r is the tip radius of curvature (cm), L is the protruding length of the emitter (cm), G ($G = L + g$, g the tip–anode distance) the inter-electrode distance (cm), A is the emission area (cm^2) and:

$$\ln\frac{I}{V^2} = \left(-6.79 \times 10^7 \Phi^{3/2}\alpha r\right)\frac{1}{V} - \ln\frac{\alpha^2 r^2 \Phi}{1.54 \times 10^{-6} A}, \tag{3}$$

where a is a parameter determined by local geometric and electronic factors $a = G/L$.

From (2), the emission current changes with the inter-electrode gap G as:

$$\frac{\partial I}{\partial G} = \left(-3.08 \times 10^{-6}\frac{AL^2V^2}{G^3r^2\Phi} - 104.57\frac{ALV^2\Phi^{1/2}}{G^2r}\right) \times \exp\left(-6.79 \times 10^7 \frac{\Phi^{3/2}Gr}{VL}\right). \tag{4}$$

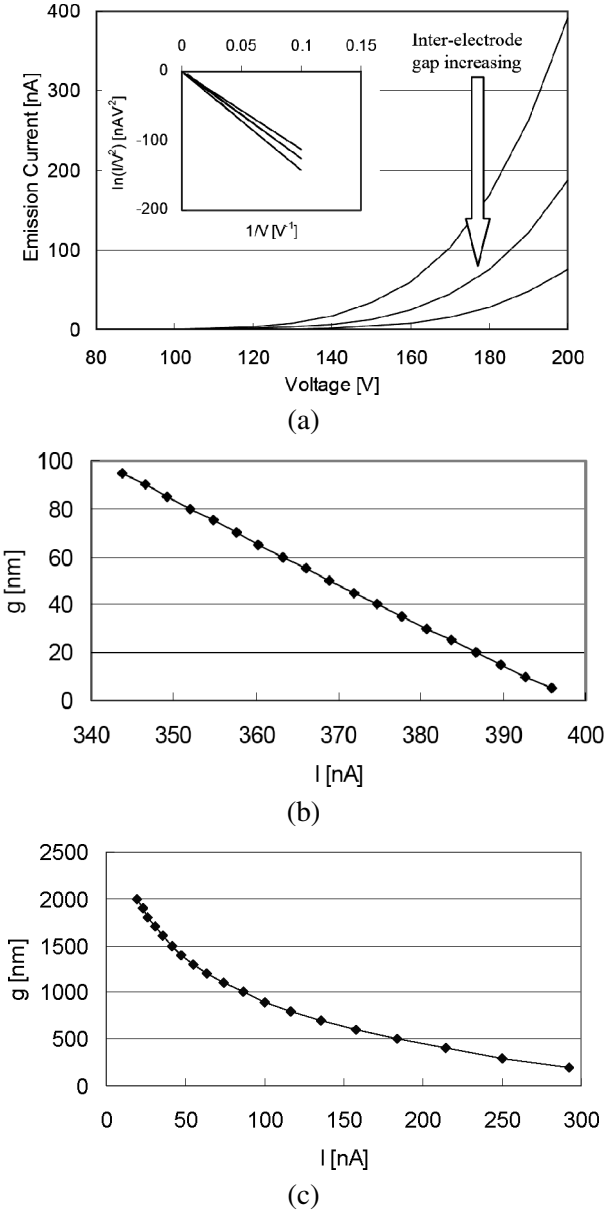

Figure 3. Vertical position sensing. (a) Simulation of the field emission of a tube of 5 μm height and 15 nm radius for different inter-electrode distances: 100, 500, and 1000 nm with inset showing the F–N plots with different inclination. (b) Change of current in a 'near-field' with inter-electrode distances smaller than 100 nm. (c) Change of current in a 'far-field' with inter-electrode distances of 100–2000 nm.

From (1) and (3) and for field emission ($G > L$) in the 'near-field', i.e., $G \approx L$ or $\alpha = G/L \approx 1$, I becomes maximum and is inversely proportional to G so

(a)

(b)

Figure 4. Analysis of electric field for vertical position sensing for an anode probe with 200-nm tip radius and nanotubes of 30 nm in diameter and 1 μm in length for different inter-electrode distances: (a) 400, (b) 600 and (c) 800 nm using ANSYS 9.0.

that better resolution is obtained. In a F–N plot, this means a large inclination (see (2) for the coefficient of $1/V$). On the other hand, in a far field as $G \gg L$ or $\alpha = G/L \gg 1$, the resolution becomes worse (Fig. 3). Experiments in Ref. [11]

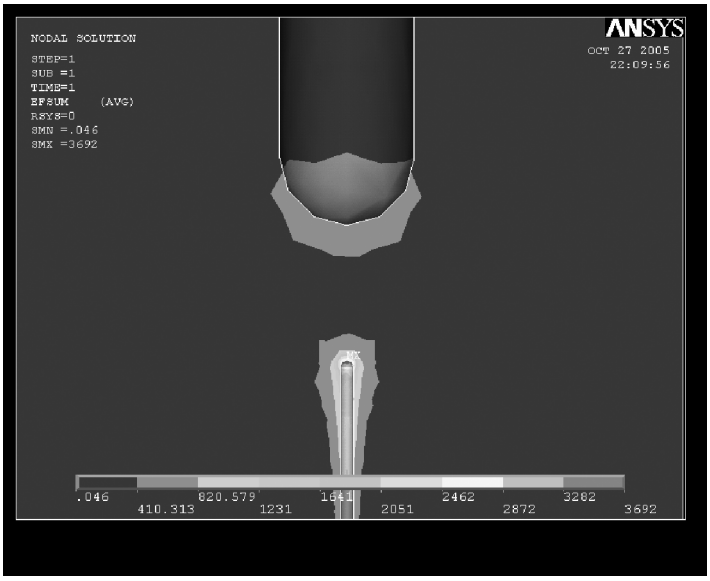

(c)

Figure 4. (Continued).

show that it is possible to obtain a 100-nm resolution at room temperature inside 10^{-4} Pa vacuum. Higher resolution can be obtained by stabilizing the emission current by baking the nanotube emitters and working at lower temperatures and/or in higher vacuum.

The field emission current is also affected by the shape of the anode. Finite element methods were used to investigate enhancements to the local field when the scanning anode is represented as a cylindrical probe with a semispherical tip. ANSYS 9.0 was employed to analyze the electric field for an anode probe with a 200 nm tip radius, and nanotubes of 30–50 nm diameter and 1–5 μm length for different inter-electrode distances (0.4–1.4 μm). Figure 4 shows the results for a tube with a 30 nm diameter and 1 μm length for different inter-electrode distances (400, 600, and 800 nm) under a 300-V bias voltage. The maximum field is found to be 3692 V/μm, giving an enhancement factor of 4.9 by noting that the nominal field is 750 V/μm for an inter-electrode distance of 400 nm.

3.3. Lateral position sensing

The lateral offset between a nanotube emitter and the scanning anode will influence both the strength and the distribution of the electric field. ANSYS 9.0 is again applied for analyzing the electric field for an anode probe with a 200-nm tip radius, and nanotubes of 30–50 nm diameter and 1–5 μm length for different lateral offsets of 0–2 μm. Figure 5 shows the results for a tube of 30 nm diameter, 1 μm length, and lateral offsets of 0, 500 and 1000 nm under a 300-V bias voltage. A constant 400-nm inter-electrode distance in the vertical direction was maintained.

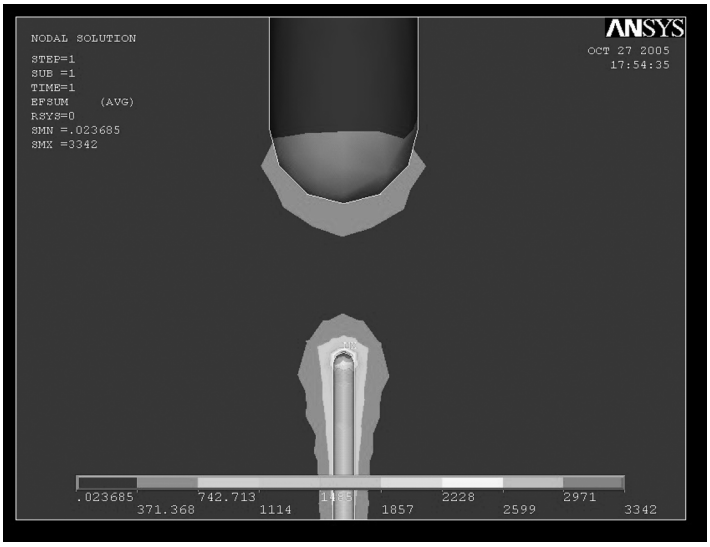

(a)

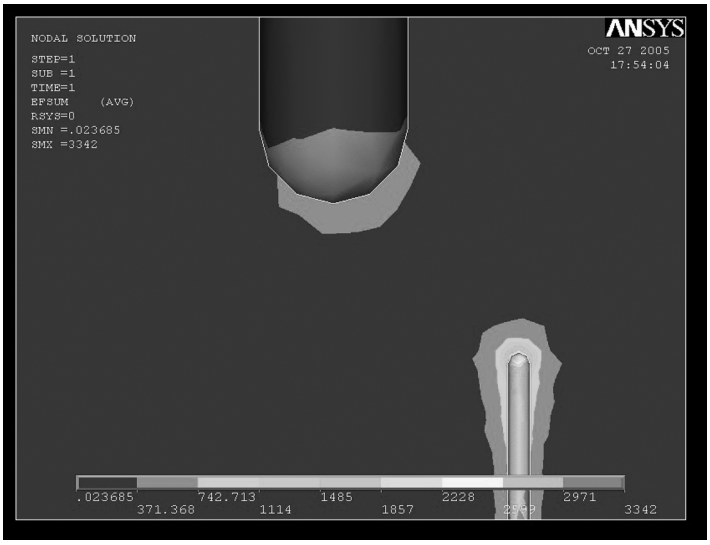

(b)

Figure 5. Analysis of electric field for horizontal position sensing for an anode probe with 200-nm tip radius and nanotubes of 30 nm in diameter and 1 μm in length for different lateral offsets: (a) 0, (b) 500 and (c) 1000 nm using ANSYS 9.0.

Simulation has shown that the field enhancement factor also changes with emitter density and that current density is a function of the distance between nanotube emitters [17]. Experimental investigation of single nanotube arrays with a scanning anode has verfied this [13]. This suggests the possibility of detecting the lateral position of a scanning anode by monitoring the emission current.

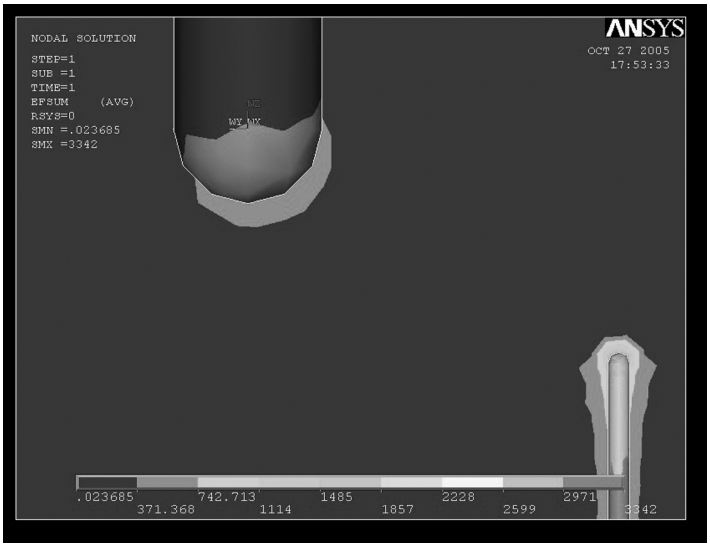

(c)

Figure 5. (Continued).

Contrary to intuition, the optimal lateral sensing resolution of the nano encoder is not realized by decreasing the space between nanotubes, because it has been recognized that arrays of closely spaced nanotubes have lower field enhancement factors than sparse arrays due to field shielding, as illustrated in Fig. 6 [13]. The nanotube spacing distance H and the nanotube height L are critical to the field enhancement factor. When nanotubes are far apart, field enhancement is strong, but the total number of emitters per unit area is low, which reduces the emitted current. When nanotubes are closely spaced, they shield one another, thus reducing the field enhancement factor. At H/L approx. 2, an optimal spacing is reached where the field is only minimally reduced by the neighboring nanotubes and their numbers per unit area remain high. Therefore, to produce the most effective field emission cathodes, patterned arrays of nanotubes at controlled spacing must be created.

4. SCANNING ANODE FIELD EMISSION PROBE

A nanomanipulator (MM3A; Kleindiek) installed inside a scanning electron microscope (SEM) (Carl Zeiss; DSM962) is used for the experiments. The manipulator (as shown in Fig. 7) has 3 d.o.f. of freedom and nanometer to subnanometer scale resolution (Table 1). The manipulator is used to control the relevant position and orientation of a scanning anode to the emitter array fixed on the sample holder of the SEM. In the experiments, the manipulator and the Si substrate with the nanotube array is configured as shown in Fig. 8. Calculations show that as moving/scanning in A/B direction by joint q_1/q_2, the additional linear motion in the C direction is very small. For example, when the arm length is 50 mm, the additional motion in

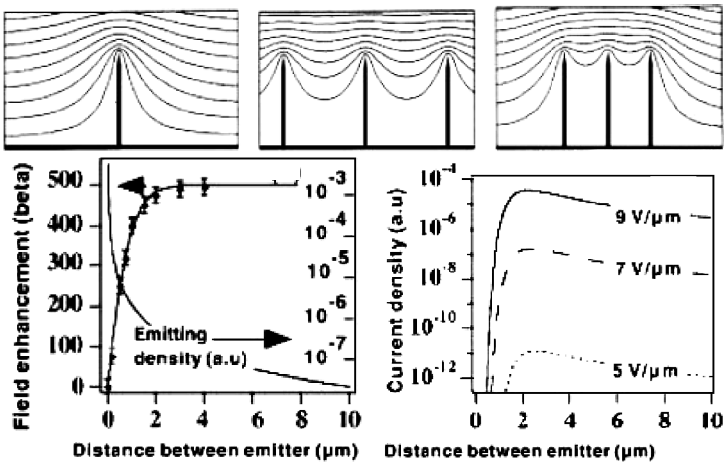

(a)

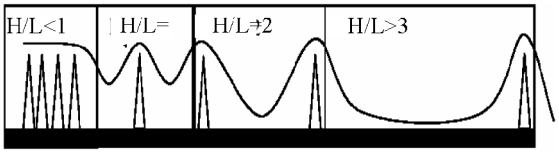

(b)

Figure 6. Horizontal position sensing. (a) Simulation of the equipotential lines of the electrostatic field for tubes of 1 μm height and 2 nm radius, for distances between tubes of 4, 1 and 0.5 μm, along with the corresponding changes of the field enhancement factor band emitter density and current density as a function of the distance (from Ref. [17]). (b) Field enhancement profile for different ratios of tube spacings and height (from Ref. [13]).

the C direction is only 0.25–1 nm when moving in the A direction for 5–10 μm; these errors can be ignored or compensated for with an additional motion of the prismatic joint p_3, which has a 0.25-nm resolution.

Fundamental field emission properties of a single nanotube in a 10-μm spacing array show the as-grown nanotubes exhibit typical I–V and F–N curves, as shown in Fig. 9.

5. THREE-DIMENSIONAL POSITION SENSING

5.1. Vertical position sensing

Vertical position sensing has been calibrated by a scanning anode actuated in the C direction of the manipulator (as shown in Fig. 10), which has a 0.25-nm resolution. The anode probe is first aligned to the tube and then moves towards the tube tip until a contact occurs. Resistance is measured to monitor the conductance. The probe is then moved away from the tube, and pulses are countered to determine the distance between the tip and the probe at higher resolutions than

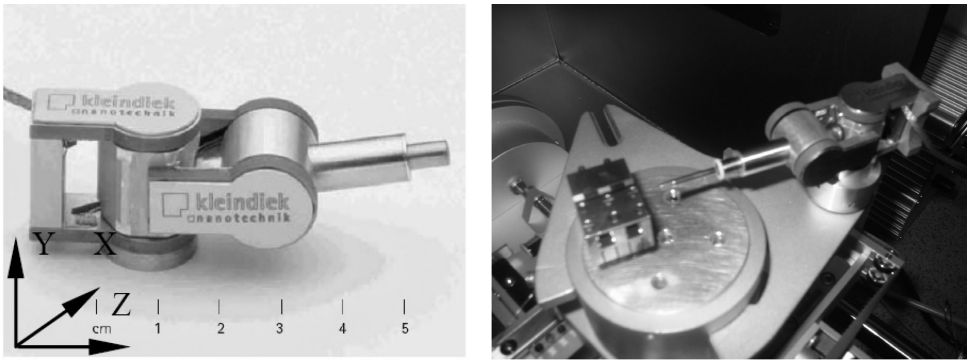

(a) MM3A (b) Installation

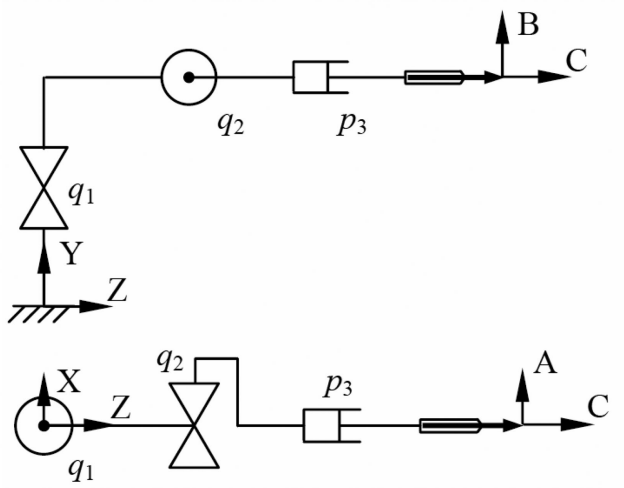

(c) Kinematic model

Figure 7. Nanomanipulator (MM3A; Kleindiek) inside a SEM.

Table 1.
Specifications of MM3A

Operating range q_1 and q_2	240°	Operating range Z	12 mm
Resolution A (horizontal)	10^{-7} rad (5 nm)	Resolution B (vertical)	10^{-7} rad (3.5 nm)
Resolution C (linear)	0.25 nm	Fine (scan) range A	20 μm
Fine (scan) range B	15 μm	Fine (scan) range C	1 μm
Speed A, B	10 mm/s	Speed C	2 mm/s

SEM micrographs provide. The manipulator is stopped at certain positions and the emission current is measured by sweeping the voltage from 0 to 475 V. I–V curves for the distances of 488, 549, 791, 1005, 1222 and 1398 nm are shown in Fig. 11.

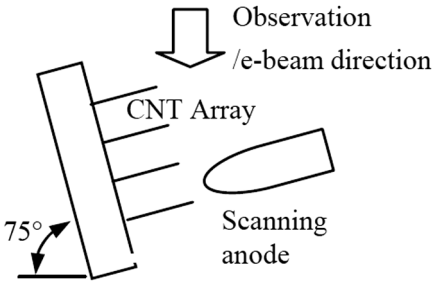

(a)

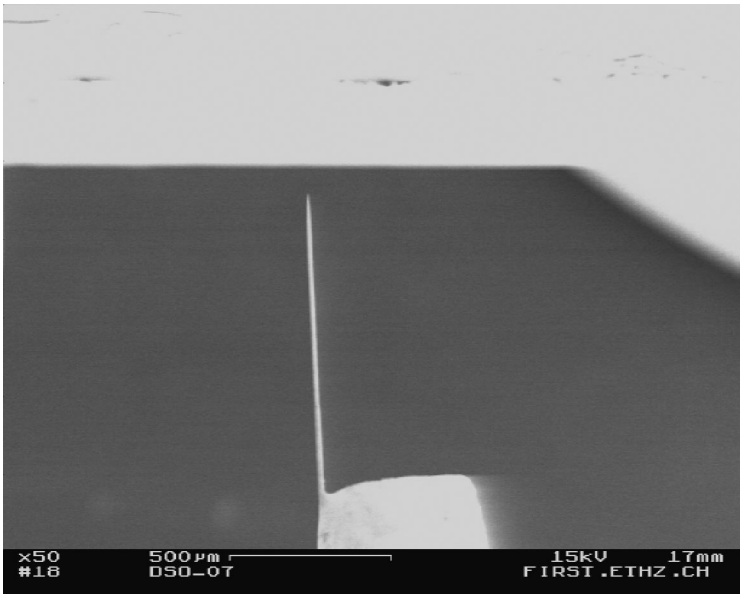

(b)

Figure 8. Configuration of scanning anode and Si substrate with MWNT array.

The measurement was performed at room temperature in an SEM vacuum chamber (vacuum is about 10^{-6} Torr). It can be seen from Fig. 11a that the resolution is a function of inter-electrode distance and applied voltages, and that the higher the voltage, the larger the difference between curves. The linearity at approximately a 450-V bias is shown in Fig. 11b. Constant voltage mode can be used. Figure 11c shows the relationship between emission current and the inter-electrode distance, suggesting that a sub-100-nm (98.3-nm for the worst case) resolution is possible for vertical position sensing. Rresolution could be further improved by stabilizing the current and compensating for thermal drift and length diversity of individual emitters in an entire array.

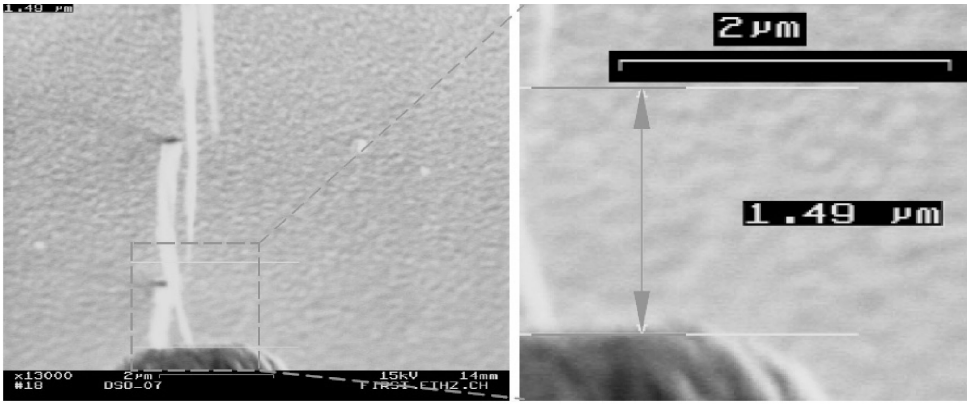

(a)

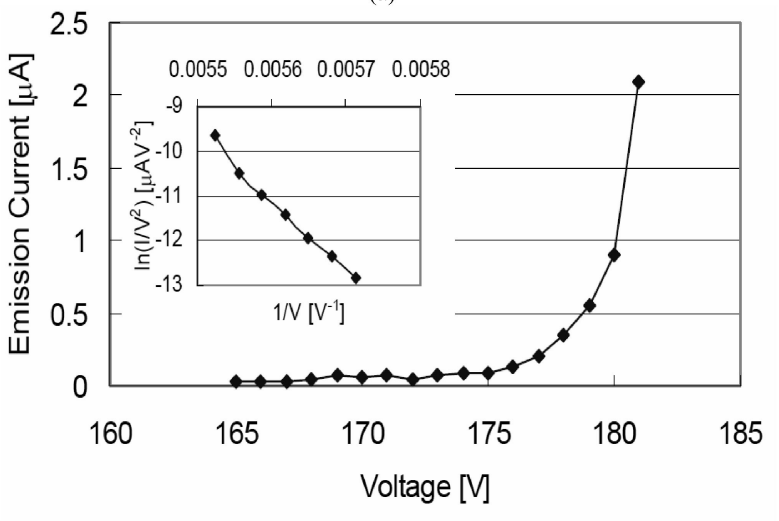

(b)

Figure 9. Fundamental field emission properties of a single nanotube array. (a) Nanotube emitter. (b) I–V curve and F–N plot (Inset).

5.2. Horizontal position sensing

Lateral position sensing has been calibrated by the same scanning anode actuated in the A direction of the manipulator (as shown in Fig. 12), which has a 5-nm resolution. The original position of the anode probe is determined as described above. Then, the probe is moved away from the tube vertically as when scanning in the lateral direction. The emission current is measured by sweeping the voltage from 0 to 200 V. I–V curves for the lateral distances of 0, 972, 1496 and 2221 nm are shown in Fig. 13. The measurement was performed at room temperature in the SEM vacuum chamber (vacuum approximately 10^{-6} Torr). It can be seen from Fig. 13a and b that the current is a function of the lateral distance. Figure 13c is the same

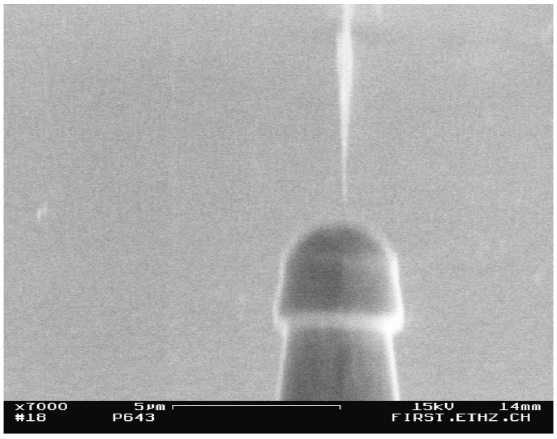

(a)

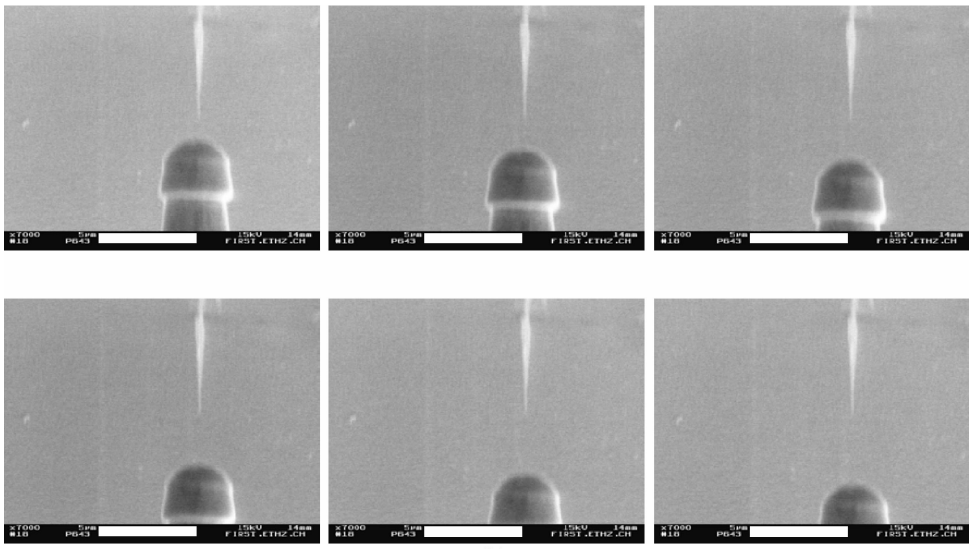

(b)

Figure 10. Vertical position sensing (scale bars: 5 μm).

curve as shown in Fig. 13b, but with nearby tubes shown. The sharp change suggests a very high resolution is possible for lateral position sensing around a nanotube, but for farther distances, no emission current was detected. At 150 V, a resolution of 38.0 nm was obtained by setting the current drift at 1 nA. A higher voltage brings about a higher resolution. The best resolution of 12.9 nm under 155 V was achieved, but a risk of damage due to current saturation then exists. Further investigation will focus on optimizing the current distribution using tube arrays with different spacing and scanning an entire array.

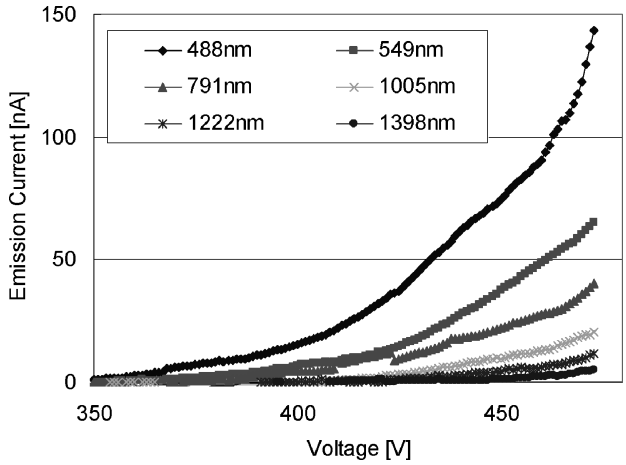

(a)

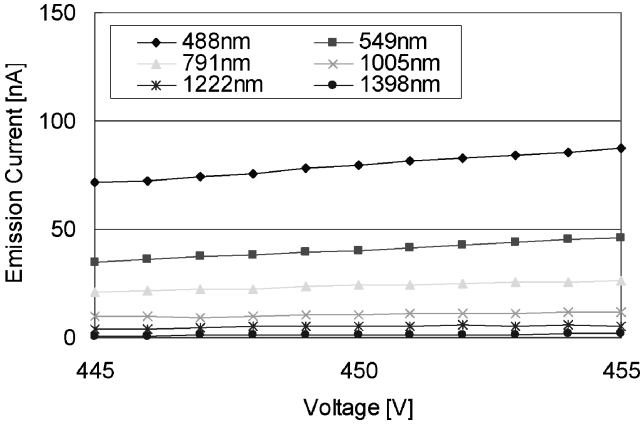

(b)

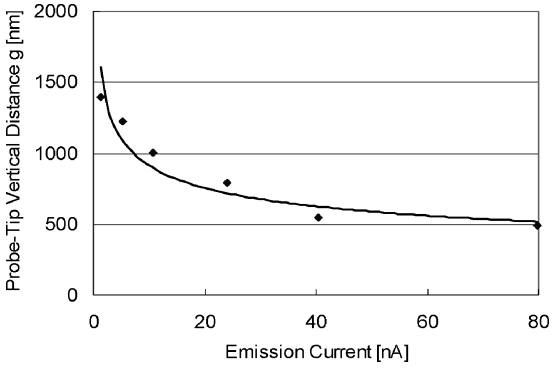

(c)

Figure 11. Vertical position sensing. (a) I–V curves for inter-electrode distances: 488, 549, 791, 1005, 1222 and 1398 nm. (b) I–V curves around 450 V. (c) Relationship between emission current and the inter-electrode distance under a constant voltage of 450 V.

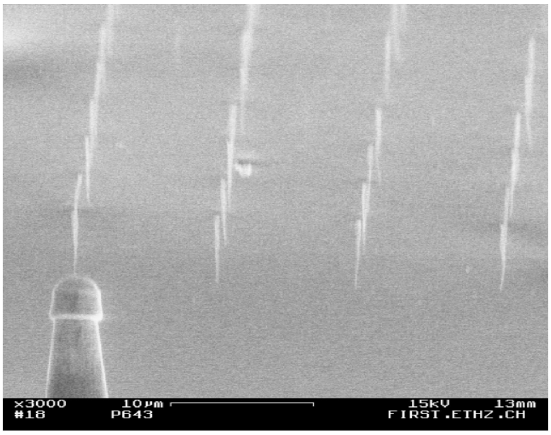

(a)

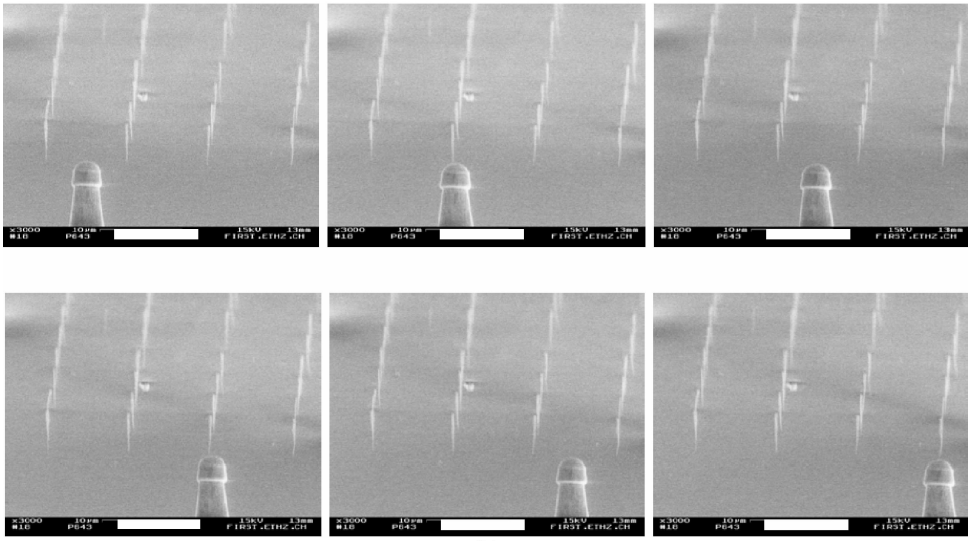

(b)

Figure 12. Lateral position sensing (scale bars: 10 μm).

6. CONCLUSIONS

Single MWNT array-based linear nano encoders have been investigated from experimental, theoretical and design perspectives. Vertically aligned single MWNTs have been realized using a combination of EBL and PECVD growth. EBL is used to define 50- to 150-nm nickel catalyst dots at precise locations on a silicon chip. Precise control of the position, density and alignment of the tubes has been achieved. Aligned nanotube arrays with spacing varying from 250 nm to 25 μm are realized. Field emission properties of the array are investigated using a scanning anode actuated with a 3-d.o.f. nanorobotic manipulator with nanometer resolution inside

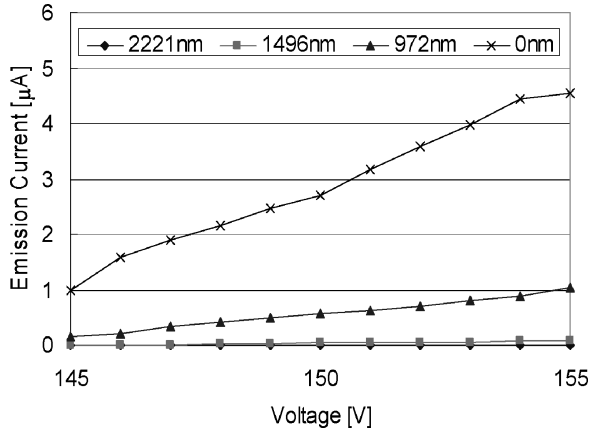

(a)

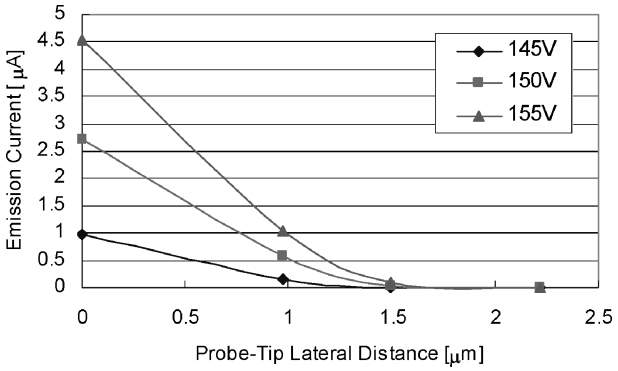

(b)

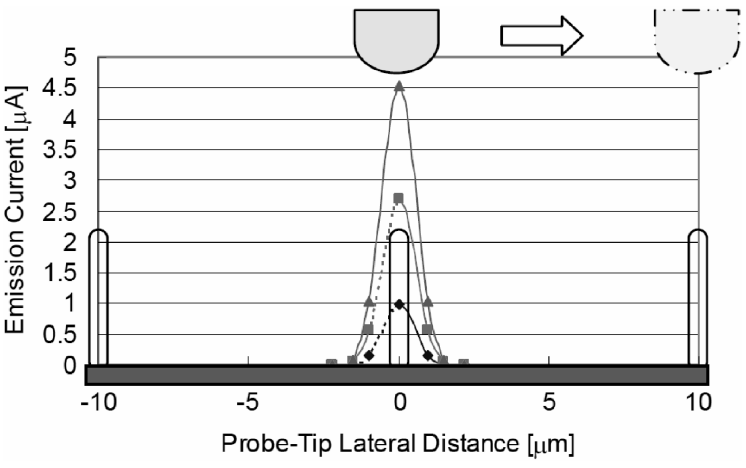

(c)

Figure 13. Lateral position sensing. (a) I–V curve. (b) Relationship between emission current and lateral distance under different bias. (c) The same curve as shown in (b), but with nearby tubes shown.

a SEM. Vertical and lateral positions have been detected by monitoring the emission current change. A resolution of 98.3 nm in the vertical direction and 38.0 nm (best: 12.9 nm) in the lateral direction has been achieved.

REFERENCES

1. V. Balzani, M. Venturi and A. Credi, *Molecular Devices and Machines: A Journey into the Nanoworld*. Wiley-VCH, Weinheim (2003).
2. K. E. Drexler, *Nanosystems: Molecular Machinery, Manufacturing, & Computation*. Wiley, New York (1992).
3. A. M. Fennimore, T. D. Yuzvinsky, W.-Q. Han, M. S. Fuhrer, J. Cumings and A. Zettl, Rotational actuators based on carbon nano-tubes, *Nature* **424**, 408–410 (2003).
4. L. X. Dong, B. J. Nelson, T. Fukuda and F. Arai, Towards linear nano servomotors with integrated position sensing, in: *Proc. IEEE Int. Conf. on Robotics & Automation*, Barcelona, pp. 867–872 (2005).
5. G. Binnig, H. Rohrer, C. Gerber and E. Weibel, Surface studies by scanning tunneling microscopy, *Phys. Rev. Lett.* **49**, 57–61 (1982).
6. G. Binnig, C. F. Quate and C. Gerber, Atomic force microscope, *Phys. Rev. Lett.* **56**, 93–96 (1986).
7. P. Liu, L. X. Dong, T. Fukuda, F. Arai, M. Nagai and Y. Imaizumi, Carbon nanotubes based position sensors, in: *Proc. Int. Conf. on Intelligent Mechatronics and Automation*, Chengdu, pp. 12–17 (2004).
8. A. Hansson and S. Stafstro, Intershell conductance in multiwall carbon nanotubes, *Phys. Rev. B* **67** (2003).
9. W. Zhu, C. Bower, O. Zhou, G. Kochanski and S. Jin, Large current density from carbon nanotube field emitters, *Appl. Phys. Lett.* **75**, 873–875 (1999).
10. D. Y. Zhong, G. Y. Zhang, S. Liu, T. Sakurai and E. G. Wang, Universal field-emission model for carbon nanotubes on a metal tip, *Appl. Phys. Lett.* **80**, 506–508 (1999).
11. F. Arai, P. Liu, L. X. Dong and T. Fukuda, Field emission property of individual carbon nanotubes and its applications, in: *Proc. IEEE Int. Conf. on Robotics & Automation*, New Orleans, LA, pp. 440–445 (2004).
12. L. X. Dong, F. Arai, T. Fukuda and B. J. Nelson, Field emission of telescoping multi-walled carbon nanotubes, in: *Proc. 4th IEEE Int. Conf. on Nanotechnology*, Munich (2004).
13. V. Semet, V. T. Binh, P. Vincent, D. Guillot, K. B. K. Teo, M. Chhowalla, G. A. J. Amaratunga, W. I. Milne, P. Legagneux and D. Pribat, Field electron emission from individual carbon nanotubes of a vertically aligned array, *Appl. Phys. Lett.* **81**, 343–345 (2002).
14. D. Carnahan, M. Reed, Z. Ren and K. Kempa, Field emission from arrays of carbon nanotubes, available online at http://www.nano-lab.com.
15. R. H. Fowler and I. W. Nordheim, Field emission in intense electric fields, *Proc. R. Soc. London Ser. A* **119**, 173–181 (1928).
16. W. A. de Heer, A. Chatelain and D. Ugarte, A carbon nanotube field-emission electron, *Science* **270**, 1179–1180 (1995).
17. L. Nilsson, O. Groening, C. Emmenegger, O. Kuettel, E. Schaller, L. Schlapbach, H. Kind, J.M. Bonard and K. Kern, Scanning field emission from patterned carbon nanotube films, *Appl. Phys. Lett.* **76**, 2071–2073 (2000).

ABOUT THE AUTHORS

Lixin Dong received the BS and MS degrees in Mechanical Engineering from Xi'an University of Technology, PRC, in 1989 and 1992, respectively, and the DE degree in Micro System Engineering from Nagoya University, Nagoya, Japan, in 2003. He was with the Department of Mechanical Engineering, Xi'an University of Technology, as a Research Associate from 1992 to 1995, as a Lecturer from 1995 to 1998 and, since 1998, he has been an Associate Professor. In 1995, he was a Visiting Researcher in the Department of Mechanical Engineering, Fukui University, Fukui, Japan. From 2003 to 2004, he was an Assistant Professor in the Department of Micro-Nano Systems Engineering, Nagoya University. He is currently a Senior Research Scientist in the Institute of Robotics and Intelligent Systems, Swiss Federal Institute of Technology, Zurich. His primary research direction lies in nanorobotics including nanorobotic manipulation and related technologies such as science and engineering of carbon nanotubes, nanofabrication, nanoassembly and nanoelectromechanical systems.

Arunkumar Subramanian is currently pursuing his PhD degree at the Institute of Robotics and Intelligent Systems (IRIS), ETH Zurich. Prior to joining IRIS, he was a Scientist at the Honeywell Laboratories in Plymouth, MN, USA, working on microelectromechanical systems (MEMS) and MEMS-enabled technologies. He received his BE degree in Mechanical and Electrical Engineering from Birla Institute for Technology and Science, India, in 1999, and his MS degree in Mechanical Engineering from the University of Minnesota, in 2002. His research interests are in the areas of nanoelectromechanical systems, MEMS, carbon nanotubes (CNTs), nanofabrication and nanomachining. His current efforts are focused on developing novel batch fabrication techniques to realize CNT-based nanostructures for nanoscale transduction.

Daniel Hugentobler was born in Bern in 1979. At 16 years he moved to Basel for 3 years and became a Laboratory Assistant of chemistry. Aftrewoods he moved back to Bern and passed the Gymnasium. Then he moved to Zürich to study Mechanical Engineering. In 2006 he finished the Master degree course. The master work was written at Nagoya University in the field of carbon nanocoils.

Bradley J. Nelson received the BS degree in Mechanical Engineering from the University of Illinois at Urbana-Champaign in 1984, the MS degree in Mechanical Engineering from the University of Minnesota, Minneapolis, in 1987, and the PhD degree in Robotics from the School of Computer Science, Carnegie Mellon University, Pittsburgh, PA, in 1995. During these years, he was also an Engineer with Honeywell, Minneapolis, MN, and Motorola, Bothell, WA, and was a US Peace Corps Volunteer, Botswana, Africa. In 1995, he became Assistant Professor with the University of Illinois at Chicago, Associate Professor at the University of Minnesota in 1998 and Professor at ETH Zürich, Switzerland, in 2002, where he is currently the Director of IRIS and Head of the Department of Mechanical and Process Engineering (D-MAVT). His primary research direction is in extending robotics research into emerging areas of science and engineering. His most recent scientific contributions have been in the area of microrobotics, biomicrorobotics and nanorobotics, including efforts in robotic micromanipulation, microassembly, microelectromechanical systems (sensors and actuators), mechanical manipulation of biological cells and tissue, and nanoelectromechanical systems. He has also contributed to the fields of visual

servoing, force control, sensor integration, and web-based control and programming of robots. He has been awarded a McKnight Land-Grant Professorship and is a recipient of the Office of Naval Research Young Investigator Award, the National Science Foundation Faculty Early Career Development (CAREER) Award, the McKnight Presidential Fellows Award and the Bronze Tablet. He was elected as a Robotics and Automation Society Distinguished Lecturer in 2003 and received the Best Conference Paper Award at the IEEE 2004 International Conference on Robotics and Automation. He was named to the 2005 '*Scientific American 50*', *Scientific American* magazine's annual list that recognizes outstanding acts of leadership in science and technology from the past year. He serves on or has been a member of the editorial boards of the *IEEE Transaction on Robotics*, *Journal of Micromechatronics*, *The Journal of Optomechatronics* and *IEEE Robotics and Automation Magazine*. He has chaired several international workshops and conferences.

Yu Sun is Assistant Professor of Mechanical and Industrial Engineering Department, and is jointly appointed in the Institute of Biomaterials and Biomedical Engineering and Electrical and Computer Engineering Department at the University of Toronto. He received the BS degree in Electrical Engineering from Dalian University of Technology, PRC, in 1996, the MS degree from the Institute of Automation, Chinese Academy of Sciences, Beijing, PRC, in 1999, the MS degree in Electrical Engineering from the University of Minnesota, in 2001, and the PhD degree in mechanical engineering from the University of Minnesota, in 2003. He held a Research Scientist position at the Swiss Federal Institute of Technology (ETH Zurich) before joining the faculty of the University of Toronto. His research areas are microelectromechanical systems design, fabrication and testing, microrobotic manipulation of biomaterials, cellular biomechanics, nanofabrication, and nanorobotic manipulation of nanomaterials.